Award Number:
W81XWH-13-1-0442

TITLE:
Targeting Ovarian Cancer with Porphysome Nanotechnology

PRINCIPAL INVESTIGATOR:
Gang Zheng

CONTRACTING ORGANIZATION: University Health Network
Toronto, ON, Canada
M5G 2C4

REPORT DATE: October 2016

TYPE OF REPORT: Annual

PREPARED FOR: U.S. Army Medical Research and Materiel Command
Fort Detrick, Maryland 21702-5012

REPORT DOCUMENTATION PAGE

Form Approved
OMB No. 0704-0188

1. REPORT DATE *(DD-MM-YYYY)*	**2. REPORT TYPE**	**3. DATES COVERED** *(From - To)*
October 2016	Annual	30Sep2015 - 29Sep2016

4. TITLE AND SUBTITLE
Targeting Ovarian Cancer with Porphysome Nanotechnology

5a. CONTRACT NUMBER
W81XWH-13-1-0442

5b. GRANT NUMBER
W91ZSQ9277N522

5c. PROGRAM ELEMENT NUMBER

6. AUTHOR(S)

Gang Zheng; Michael S. Valic, Chris Zhang, Wenlei Jiang, Lili Ding, Juan Chen, Marcus Q. Bernardini

Email: gang.zheng@uhnresearch.ca

5d. PROJECT NUMBER

5e. TASK NUMBER

5f. WORK UNIT NUMBER

7. PERFORMING ORGANIZATION NAME(S) AND ADDRESS(ES)

University Health Network
200 Elizabeth Street
Toronto, ON, Canada
M5G 2C4

8. PERFORMING ORGANIZATION REPORT NUMBER

9. SPONSORING / MONITORING AGENCY NAME(S) AND ADDRESS(ES)
U.S. Army Medical Research and Materiel Command
Fort Detrick, Maryland 21702-5012

10. SPONSOR/MONITOR'S ACRONYM(S)

11. SPONSOR/MONITOR'S REPORT NUMBER(S)

12. DISTRIBUTION / AVAILABILITY STATEMENT
Approved for public release; distribution unlimited

13. SUPPLEMENTARY NOTES

14. ABSTRACT

Purpose: The Porphysome is a *first-in-class* porphyrin-based nanotheransotic with inherent biophotonic, photo-physical, and metal chelation properties that can be exploited for multi-modal imaging *in Vivo*. Herein we report preliminary preclinical data of the use of systemically administered non-targeted Porphysomes for the detection of orthotopic ovarian lesions.

Methods: Two ovarian tumour xenograft models are established with human SK-OV-3 and OV-90 cell lines installed into one ovary (orthotopic) of athymic (*Nu/Nu*) mice. Upon reaching 3.5 mm tumour size, mice are administered non-targeted Porphysome nanovesicles (intravenous, bolus, ~10 mg kg^{-1} porphyrin dose). Mice are divided into two treatment groups receiving either unlabelled Porphysomes or positron-emitting Copper-64 (^{64}Cu)-labelled Porphysomes (^{64}Cu-Porphysomes). Sham surgical controls and vehicle controls are included. 24-hours post-injection the mice receiving Porphysomes are sacrificed and tissue biodistribution performed using *ex Vivo* tissue homogenate fluorescence. The mice receiving ^{64}Cu-Porphysomes are sacrificed and tissue biodistribution performed using *ex Vivo* tissue gamma (γ)-counting.

Results: Quantification of ^{64}Cu signal (γ-counting) revealed insignificant differences in the accumulation of non-targeted ^{64}Cu-Porphysomes in ovarian lesions versus healthy ovaries. Quantification of porphyrin fluorescence (tissue homogenate fluorescence) also revealed insignificant differences in Porphysome accumulation. Taken together, these preliminary data suggest that non-targeted Porphysomes relying solely on passive mechanisms for accumulation (e.g., enhanced permeability and retention (EPR)-effect phenomena) is an inadequate strategy for yielding significant accumulation and retention of Porphysomes in malignant ovarian tissues compared with healthy ovarian tissues.

Conclusion: Quantifying the differences in the tissue biodistribution of systemic administered non-targeted Porphysomes revealed inadequate accumulation and retention of Porphysomes in ovarian lesions. These preliminary data motivate the continued development of active targeting strategies with folate receptor (FR) targeted Porphysome formulations (Fol-Porphysomes) in order to specifically enhance their accumulation and retention in FR over-expressing ovarian lesions for sensitive and specific dual-modal imaging of advanced solid tumours, and for future applications in drug delivery.

15. SUBJECT TERMS
Nanomedicines; Porphyrin; Fluorescence Image Guided Surgery; Biodistribution; Ovarian Cancer; Preclinical Models.

16. SECURITY CLASSIFICATION OF:			**17. LIMITATION OF ABSTRACT**	**18. NUMBER OF PAGES**	**19a. NAME OF RESPONSIBLE PERSON**
					USAMRMC
a. REPORT	**b. ABSTRACT**	**c. THIS PAGE**	UU	16	**19b. TELEPHONE NUMBER** *(include area code)*
U	U	U			

Standard Form 298 (Rev. 8-98)
Prescribed by ANSI Std. Z39.18

Table of Contents

Introduction:

Ovarian cancer (OC) is the fifth most diagnosed cancer in women and second most frequent invasive malignancy of the female genital tract—with an estimated 26,000 cases diagnosed annually between the U. S. and Canada. Approximately 15,000 women die each year from OC in the U. S., casting OC as the most common cause of death among women with gynaecologic malignancies. Early detection is the key to the successful treatment of OC; however, less than 20% of all OCs are found at an early enough stage to permit curative treatments because the disease causes few specific symptoms when it is localized to the ovary. As a result, almost 75% of women continue to be diagnosed with disseminated OC (e.g., stage III or IV), with a resultant 5-year survival rate of only 15%. This poor overall survival has remained essentially unchanged over the past 20 years, despite advances in surgical practices and new chemotherapies.

Operative debulking of tumours (a.k.a., cytoreduction) is a procedure whereby a surgically incurable cancer is partially removed without curative intent in order to make subsequent treatment with platinum-based chemotherapies more effective. At present, early debulking surgeries are a leading front-line treatment for advanced-disease OCs. Aggressive debulking methods involving extensive upper abdominal procedures (e.g., bowel resection, peritoneal stripping, etc.) are increasingly preferred by surgeons in order to achieve an "optimal" residual disease status—that is, leaving macroscopic residual disease of < 1 cm in diameter. Available evidence suggests smaller residual tumor size is an important prognostic factor that correlates with enhanced response to chemotherapy and improved patient survival. Unfortunately, the percentage of patients who receive an optimal debulking varies widely from 15–85% depending on imprecise factors such as patient selection, tumour location and dissemination, and surgeon expertise.

The imperfect and, arguably, ineffective surgical management of OCs has highlighted two immediate unmet needs for the improvement of cytoreductive methods: (1) adequate disease staging and treatment planning preoperative, and (2) descriptions of residual disease intraoperative. In recent years, several imaging strategies have gained widespread clinical interest as cytoreductive adjuncts, including fluorescence imaging using folate receptor-α (FR) targeted agents to provide real-time detection of residual disease and radio-labelled fluoro-deoxyglucose (^{18}F-FDG) to support preoperative radiographic disease staging with Positron Emission Tomography (PET). However, the clinical utility of many of these approaches remains stubbornly elusive owing to restrictive operative settings, imaging modality limitations, etc. To this end, we have proposed a translational strategy for a first-in-class, multifunctional porphyrin-based nanotheranostic (Porphysome; *Figure 1*) capable of multimodal PET/fluorescence imaging as a (1) stand-alone PET probe for precise OC staging and as a (2) surgical guidance tool for maximal debulking in advanced-stage OC patients.

Jon Lovell, Gang Zheng *et al.* have previously described an all-organic porphysome nanoparticle with intrinsically multimodal and activatable biophotonic properties [1]. In addition to being biodegradable and biocompatible, Porphysomes can directly and stably chelate PET radioisotope copper-64 (^{64}Cu) to serve as a highly accurate and non-invasive PET imaging tool [2]. ^{64}Cu-Porphysomes functionalized to with peptide-folate (^{64}Cu-Fol-Porphysome) has been experimentally validated for significant tumour-specific accumulation lasting 48 hours in primary OC xenografts overexpressing FR [3]. Therefore, folate-targeted ^{64}Cu-Fol-Porphysomes

with dual PET/fluorescence imaging may permit synchronous, non-invasive evaluation of patients with high FR expressing tumours for (1) the extent of tumour involvement and extra-ovarian dissemination by PET followed by (2) intraoperative fluorescent imaging to detect smaller cancerous lesions in real-time for surgical guidance.

Herein we report preliminary preclinical data on the optimization of formulating porphyrin-phospholipid nanovesicles (Porphysomes) and preliminary *in Vivo* data of non-targeted ^{64}Cu-Porphysomes in two orthotopic xenograft models of human OC.

Body:

Preparation of Porphysome Nanovesicles with Reverse-Phase Evaporation (Figure 2).

The production of Porphysomes had been previously reported, following a multistep thin film hydration (TFH) procedure commonly used for conventional liposomal preparations [1]. Briefly, dried lipidic films consisting of *pyro*pheophorbide-α–lysophosphatidylcholine conjugate (Pyro–lipid), cholesterol (Chol), and 1,2-distearoyl-*sn*-glycero-3-phosphoethanolamine-N-[methoxy (polyethylene glycol)-2000] (DSPE-mPEG$_{2000}$) in molar ratio 55, 40, and 5, respectively, are hydrated and undergo mechanical processing to obtain unilamellar vesicles. Two limitations of this conventional methodology are the use of chlorinated and organic solvents for various steps, and the lack of reproducible control over drug encapsulation efficiency. Residual or trace organic solvent present in the liposome formulation can represent a possible risk to human health depending on the type of solvent and the route of administration of the liposomes. Residual solvent can also influence the stability of the vesicle and drug entrapment. The encapsulation efficiency of hydrophilic, non-bilayer interacting drugs is generally poor, requiring additional procedural steps to actively load drug into the aqueous core of liposomes.

In order to overcome the above mentioned limitations of conventional liposomal preparations, an alternative method for preparing Porphysomes is reported using reverse-phase evaporation (REV) technique. 40 mg of Pyro–lipid with stoichiometric quantities of Chol and DSPE-mPEG$_{2000}$ was completely dissolved in 2 mL of anhydrous dichloromethane (DCM) in a 25 mL round bottom amber flask. After removal of the solvent by rotary evaporation, the resulting dried lipid Porphysome film was dissolved with 8 mL of ethanol (EtOH) and ethyl acetate (EtOAc) mixed at volume ratio 1:1. To this solution, 2 mL of phosphate buffered saline pH 7.4 (137 mM NaCl, 2.7 mM KCl, 10 mM Na_2HPO_4, 1.8 mM KH_2PO_4) was added to obtain a monophasic system with water. The organic solvents present were removed at 40 °C by rotary evaporation under reduced pressure to give the final Porphysome aqueous dispersion. The Porphysome suspension was diluted and extruded with high-pressure nitrogen gas through two stacked 25 mm diameter polycarbonate filters with fixed pore sizes. Extrusion was performed at 70 °C until a monodisperse Porphysome size distribution was obtained, about five passes. The physiochemical characteristics of the Porphysomes prepared with an REV technique are indistinguishable from Porphysomes prepared following conventional methodologies (*Tables 1,2*).

Orthotopic Xenograft Models of Human OC.

Orthotopic xenograft models of human OC were established using two cells lines, SK-OV-3 and OV-90, in female athymic (*Nu/Nu*) mice. SK-OV-3 is a multi-drug resistant cell line derived from a malignant ovarian ascitic effusion. *In Vivo* these cells form moderately well differentiated adenocarcinoma consistent with ovarian primary tumour and have been used to study drug

resistance and folic acid (folate) receptor targeting [4,5]. OV-90 is also a human ovarian surface epithelium (OSE)-cell line derived from a malignant extra-ovarian ascites [6]. Both OV-90 and SK-OV-3 cells share similar molecular expression profiles *in Vitro* and *in Vivo* [7].

Cellular suspensions (100×10^6 cell mL^{-1}) were injected into a single ovarian capsule exposed through a small lateral incision. The injection volume was approximately ~ 20 µL or about ~ 2×10^6 cells per injection. The growth of the xenograft was monitored weekly with magnetic resonance imaging (MRI). Tumours were usually identifiable on MR three weeks post-inoculation and grew at a rate of approximately ~1.0 mm per week thereafter. Upon xenograft reaching a greatest dimension of 5.0 mm, the mice were randomly assigned to treatment groups. Controls included a sham-surgical control consisting of an injection of sterile saline (0.9 % w/v NaCl) into the ovarian capsule, and a benign xenograft control consisting of an identically prepared cellular injection of normal human fibroblast (NF)-cell line isolated by our group (*Data not shown*).

Radio-labelling of Porphysome with Positron-emitting Copper-64 (^{64}Cu).
The procedure for radio-labelling Porphysome nanovesicles with positron emitter Copper-64 (^{64}Cu) had been previously reported [2]. Briefly, to 750 µL of Porphysome solution (0.67 mM porphyrin) was added between 5.0 to 6.0 mCi (185-217 MBq) of $^{64}CuCl_2$ diluted in 250 µL of 0.1 M ammonium acetate buffer pH 5.5 (100 mM NH_4OAc). The mixture was incubated at 60 °C for 30 minutes. The radio-chemical purity (RCP) or radio-labelling efficiency was assessed with instance thin layer chromatography (iTLC) and a gamma (γ)-ray scintillation counter. The acceptance criteria for RCP is not more than 10 % free $^{64}CuCl_2$. Radio-labelling efficiency typically ranged between 91.5% and 96.7% (n>10). The radio-labelled ^{64}Cu-Porphysomes were terminally sterilized with a syringe-driven 0.22 µm filter into a vial containing sterile saline (0.9% w/v NaCl) to create a unit dose suitable for parenteral administration. The physiochemical characteristics of the ^{64}Cu-Porphysomes after radio-labelling do not change substantially as is reported in *Table 2*.

Biodistribution of Porphysomes in Orthotopic Xenograft Models of Human Ovarian Cancer.
The biodistribution of ^{64}Cu-Porphysomes to the tissues of orthotopic xenograft models of human OC was evaluated at 24 hours' post-intravenous bolus administration. Five OV-90 mice (21.52 g ± 1.49) and two SK-OV-3 mice (21.39 g ± 0.3) have been included in the γ-counting biodistribution study to-date. The dimensions of the primary ovarian lesions were 5.42 mm ± 0.68 and 5.65 mm ± 1.63 for the OV-90 and SK-OV-3 groups, respectively. The administered activity of ^{64}Cu-Porphysomes was 474 µCi ± 50.9 and 544 µCi ± 131 for the OV-90 and SK-OV-3 groups, respectively. The Porphyrin dose (injection volume ~ 300 µL) was 12.24 mg kg^{-1} ± 0.91 and 12.26 mg kg^{-1} ± 0.17 for the OV-90 and SK-OV-3 groups, respectively. 24 hours' post-intravenous bolus administration, the mice were sacrificed and major organs excised for *ex vivo* quantification of ^{64}Cu with scintillation counting (*Figures 2,3*). Large accumulation of ^{64}Cu activity in the liver, kidneys, spleen, and lungs at 24 hours post intravenous administration is indicative of classical mononuclear phagocytic system (MPS) recognition and uptake [8]. No difference in the %I.D./g (*Figure 2*) of the ovarian tumour versus the contra-lateral healthy ovary was observed ($p = 0.1089$ SK-OV-3, $p = 0.4396$ OV-90). However, difference in the %I.D. (*Figure 3*) of the ovarian OV-90 tumour versus the contra-lateral healthy ovary was observed ($p = 0.0006$), but not for the ovarian SK-OV-3 tumour ($p = 0.2812$) owing to the small sample size

(n = 2). Taken together, these preliminary data illustrate that the non-targeted ^{64}Cu-Porphysome relying solely on passive mechanisms for accumulation such as the enhanced permeability and retention (EPR)-effect is an inadequate strategy for yielding significant accumulation of ^{64}Cu-Porphysomes in malignant ovarian tissues compared with healthy ovarian tissues.

Five SK-OV-3 mice (23.9 g ± 1.3) have been included in the Pyro-fluorescence biodistribution study to-date. The dimensions of the primary ovarian lesions were 3.2 mm ± 1.6. The Porphyrin dose (injection volume ~ 100 µL) was 12.0 mg kg^{-1} ± 0.7. 24 hours' post-intravenous bolus administration, the mice were sacrificed, the major organs excised, and homogenised in the presence of non-ionic surfactants (i.e., Triton X-100) to restore the 676-nm fluorescence emission peak of Pyro–lipid (*Figure 4*). Similar to experimental results from the γ-counting biodistribution, large accumulation of porphyrin fluorescence in the liver, kidneys, spleen, and lungs at 24 hours post intravenous administration was observed. No difference in the F_{AUC}/g of the ovarian SK-OV-3 tumour versus the contra-lateral healthy ovary was observed (p =0.05859).

Key Research Accomplishments:

- New reverse-phase evaporation (REV) technique for the preparation of Porphysome nanovesicles amendable to scaled-up under current good manufacturing practice (CGMP) production and efficient antineoplastic agent loading was described.
- Biodistribution of non-targeted ^{64}Cu-Porphysomes and Porphysomes was quantified in two orthotopic xenograft models of human OC with *ex Vivo* scintillation counting and with *ex Vivo* tissue fluorescence, respectively.
- Investigations underway exploring FR-targeted Fol-Porphysome formulations in two orthotopic xenograft models of human OC in order to optimise accumulation and retention for sensitive and specific dual-modal imaging, and future applications for drug delivery.

Reportable Outcomes:

- Abstract: Valic, M.S., Zhang, C., Ye, T., Jiang, W., Ding, L., Chen, J., Bernardini, M. Q., Zheng, G., "Porphyrin-based nanovesicles for dual-modal PET and optical fluorescence detection of ovarian cancers." Poster presentation, Personalizing Cancer Medicine in 2017, Feb. 2017, Toronto, Canada.

Conclusion:

Progresses have been made towards the preclinical validation of the Porphysome platform for the dual-modal imaging of advanced solid tumours in orthotopic xenograft models of human OC. Preparation of Porphysome nanovesicles with the reverse-phase evaporation (REV) technique dramatically improves the scalability of Porphysome preparations under CGMP guidelines and expands the possibilities for high-payload drug delivery of antineoplastic agents to advanced solid tumours. The preliminary biodistribution of non-targeted Porphysomes in two orthotopic xenograft models of human OC did not demonstrate statistically significant differences in the accumulation of Porphysomes in malignant ovarian lesions compared with healthy ovarian tissues when measured with γ-counting (analogous to PET imaging) and porphyrin fluorescence (analogous to fluorescence-image guided surgery). These data do, however, motivate the continued development of active targeting strategies with FR targeting (i.e., Fol-Porphysomes) in order to specifically enhance their accumulation and retention in FR over-expressing ovarian

lesions for sensitive and specific dual-modal imaging, and future applications for drug delivery.

References:

[1] J. F. Lovell, C. S. Jin, E. Huynh, H. Jin, C. Kim, J. L. Rubinstein, W. C. W. Chan, W. Cao, L. V Wang, and G. Zheng, "Porphysome nanovesicles generated by porphyrin bilayers for use as multimodal biophotonic contrast agents.," *Nat. Mater.*, vol. 10, no. 4, pp. 324–332, 2011.

[2] T. W. Liu, T. D. MacDonald, J. Shi, B. C. Wilson, and G. Zheng, "Intrinsically copper-64-labeled organic nanoparticles as radiotracers," *Angew. Chemie - Int. Ed.*, vol. 51, no. 52, pp. 13128–13131, 2012.

[3] C. S. Jin, L. Cui, F. Wang, J. Chen, and G. Zheng, "Targeting-triggered porphysome nanostructure disruption for activatable photodynamic therapy," *Adv. Healthc. Mater.*, vol. 3, no. 8, pp. 1240–1249, 2014.

[4] Jørgen, F., and Trempe, G., "New Human Tumor Cell Lines," in *Human Tumor Cells in Vitro*, Jørgen, F., Ed. New York: Plenum Press, 1975, pp. 115–159.

[5] H. S. L. Chan, G. Bradley, P. Thorner, G. Haddad, B. L. Gallie, and V. Ling, "Methods in laboratory investigation. A sensitive method for immunocytochemical detection of P-glycoprotein in multidrug-resistant human ovarian carcinoma cell lines," *Laboratory Investigation*, vol. 59, no. 6, pp. 870–875, 1998.

[6] A.-M. Mes-Masson, and D. M. Provencher, "Primary cultures of normal and tumoral human ovarian epithelium," U.S. Patent 5 710 038, Jan. 20, 1998.

[7] D. M. Provencher, H. Lounis, L. Champoux, M. Tétrault, E. N. Manderson, J. C. Wang, P. Eydoux, R. Savoie, P. N. Tonin, and A. -M. Mes-Masson, "Characterization of four novel epithelial ovarian cancer cell lines," *In Vitro Cell Dev. Biol. Anim.*, vol. 36, no. 6, pp. 357–61, 2000.

[8] K. M. Tsoi, S. A. MacParland, X.-Z. Ma, V. N. Spetzler, J. Echeverri, B. Ouyang, S. M. Fadel, E. A. Sykes, N. Goldaracena, J. M. Kaths, J. B. Conneely, B. A. Alman, M. Selzner, M. A. Ostrowski, O. A. Adeyi, A. Zilman, I. D. McGilvray, and W. C. W. Chan, "Mechanism of hard-nanomaterial clearance by the liver," *Nat. Mater.*, vol. 1, no. August, pp. 1–10, 2016.

[9] S. Wilhelm, A. J. Tavares, Q. Dai, S. Ohta, J. Audet, H. F. Dvorak, and W. C. W. Chan, "Analysis of nanoparticle delivery to tumours," *Nat. Rev. Mater.*, vol. 1, no. 5, p. 16014, 2016.

Appendices:

Table 1: Physiochemical properties of Porphysome formulations prepared with the REV technique under different organic solvent systems.

Organic Solvent	Dia. [nm]	Polydispersity† [nm]	PD Index‡	SOS$^{\alpha}$
Thin Film Hydration (TFH)	111.2 ±0.8	8.7 ±1.8	0.087 ±0.018	0.429 ±0.454
Ethanol/Ethyl acetate (1:1 v/v)	109.8 ±1.4	4.3 ±1.1	0.079 ±0.020	0.578 ±0.261
Ethanol/Ethyl acetate (1:3 v/v)	109.6 ±1.3	11.3 ±1.7	0.113 ±0.017	0.186 ±0.079

Table 1 cont'd: Physiochemical properties of Porphysome formulations prepared with the REV technique under different organic solvent systems.

Organic Solvent	Conductivity [mS cm^{-1}]	Mobility [µm cm s^{-1} V^{-1}]	Zeta Potential$^{\beta}$ [mV]	Zeta Potential Model$^{\gamma}$	Fit Error$^{\delta}$
Thin Film Hydration (TFH)	3.10 ±0.05	-0.41 ±0.13	-8.52 ±2.79	Henry	0.013457 ±0.000534
Ethanol/Ethyl acetate (1:1 v/v)	3.77 ±0.07	-0.39 ±0.14	-8.11 ±2.98	Henry	0.014906 ±0.001304
Ethanol/Ethyl acetate (1:3 v/v)	2.23 ±0.03	-0.50 ±0.13	-10.60 ±2.86	Henry	0.014543 ±0.000623

Table 2: Stability of physiochemical properties of REV Porphysomes (1:1 v/v EtOH/EtOAc) challenged with different conditions.

Condition	Dia. [nm]	Polydispersity† [nm]	PD Index‡	SOS$^{\alpha}$
30 Days' Cold-storage	109.5 ±1.3	5.0 ±0.9	0.085 ±0.019	1.282 ±0.165
Post ^{64}Cu Radio-labelling	109.4 ±2.7	5.2 ±1.8	0.096 ±0.033	1.181 ±0.702

Table 2 cont'd: Stability of physiochemical properties of REV Porphysomes (1:1 v/v EtOH/EtOAc) challenged with different conditions.

Condition	Conductivity [mS cm^{-1}]	Mobility [µm cm s^{-1} V^{-1}]	Zeta Potential$^{\beta}$ [mV]	Zeta Potential Model$^{\gamma}$	Fit Error$^{\delta}$
30 Days' Cold-storage	0.35 ±0.01	-0.85 ±0.2	-11.97 ±0.55	Henry	0.003631 ±0.000671
Post ^{64}Cu Radio-labelling	0.72 ±0.02	-0.72 ±0.2	-15.11 ±0.32	Henry	0.002710 ±0.000173

† Polydispersity, or width of the distribution, in [nm] determined using a Cumulants analysis.
‡ Polydispersity index based on a Cumulants analysis. Comparable to the distribution width divided by the mean.

[α] Sum of squares error for a Cumulants fit. A fairly good parameter (along with amplitude and baseline) for judging the "goodness" of the auto-correlation curve.

[β] Measure of electrokinetic potential in a colloidal system. Calculated using the electrophoretic mobility.

[γ] Henry's equation is the most general of the three formalisms. It includes both the Smoluchowski's and Hückel's equations as its limiting cases. If the size and iconicity of the sample are known, the Henry model is recommended.

[δ] Units of [μm cm V^{-1}].

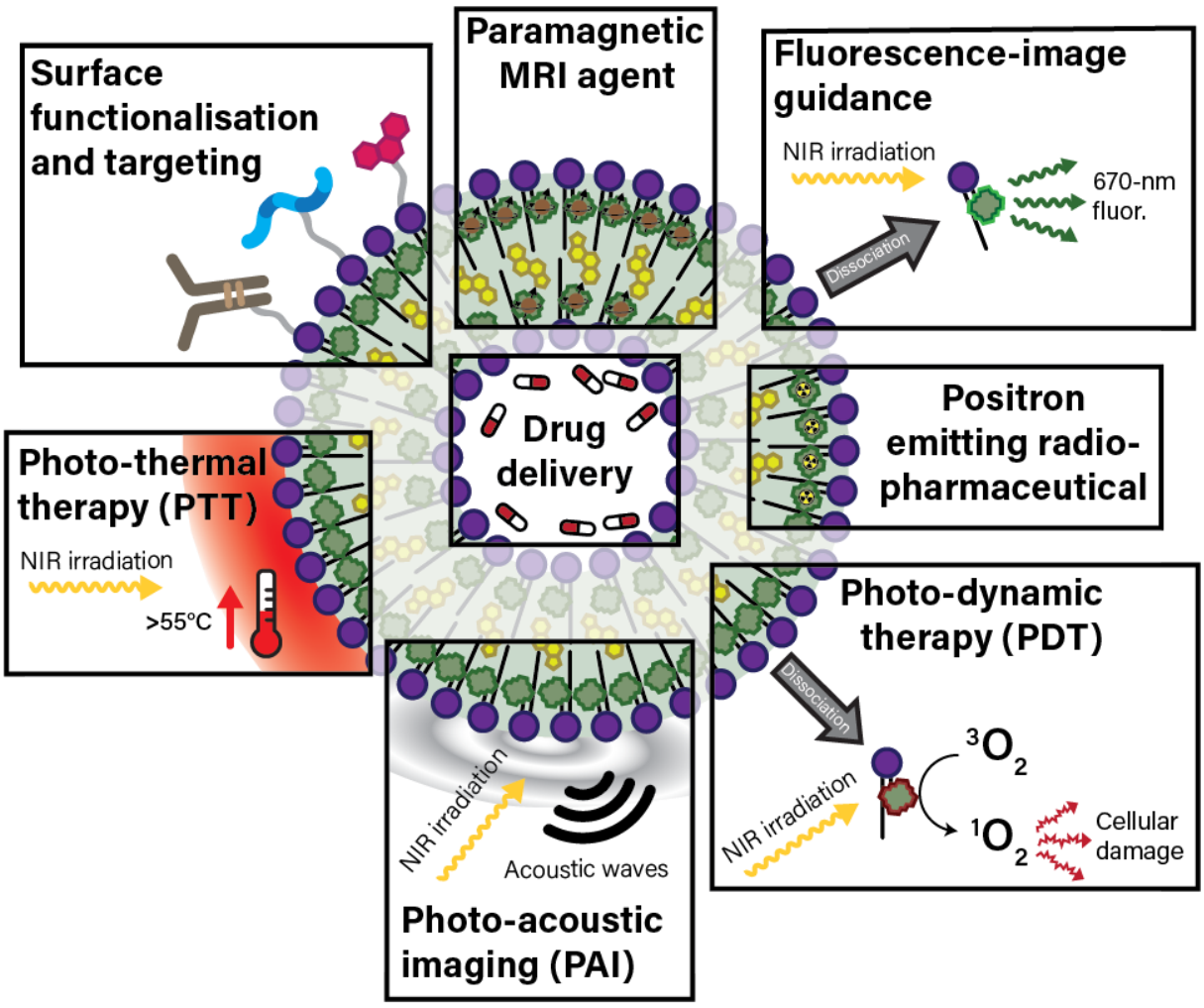

Figure 1: Overview of the multi-functional potential of the porphyrin-phospholipid bilayered structures such as the Porphysome: Targeting these nanomaterials by functionalizing with receptor ligands, antibodies, etc., chelating paramagnetic metal ions with the porphyrin building-blocks for MR imaging contrast, exploiting Porphysomes chelating abilities to serve as PET radio-tracers, and exploiting structurally dependent *modes-of-action* such as the strong absorbance of porphyrins for photothermal therapy with highly quenched, intact porphyrin-phospholipid bilayered structures and photodynamic therapy with porphyrin-phospholipid monomers following dissociation of the nanostructure.

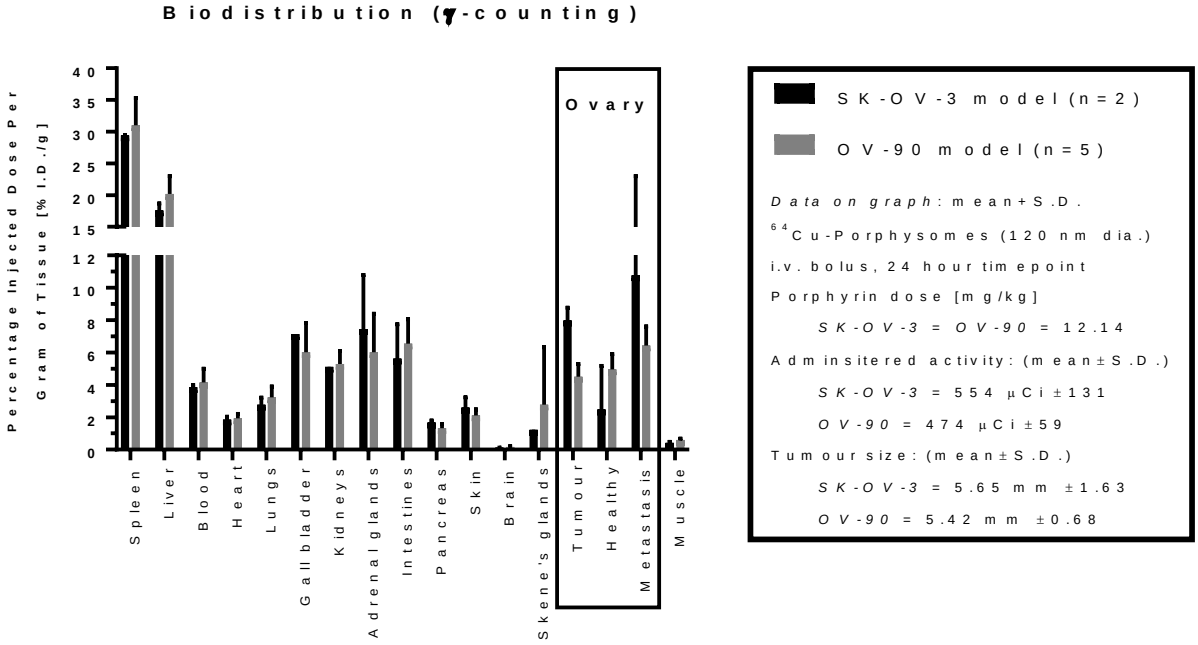

Figure 2: Biodistribution of ^{64}Cu-Porphysomes in the tissues of orthotopic xenograft models of human ovarian cancer. Each data point represents the mean + 1 standard deviation. ^{64}Cu activity was decay corrected to the time of injection and expressed as a percentage of the injected dose (%I.D.) normalized to tissue weight [g]. No difference in the %I.D./g of the ovarian tumour versus the contra-lateral healthy ovary was observed ($p = 0.1089$ SK-OV-3, $p = 0.4396$ OV-90).

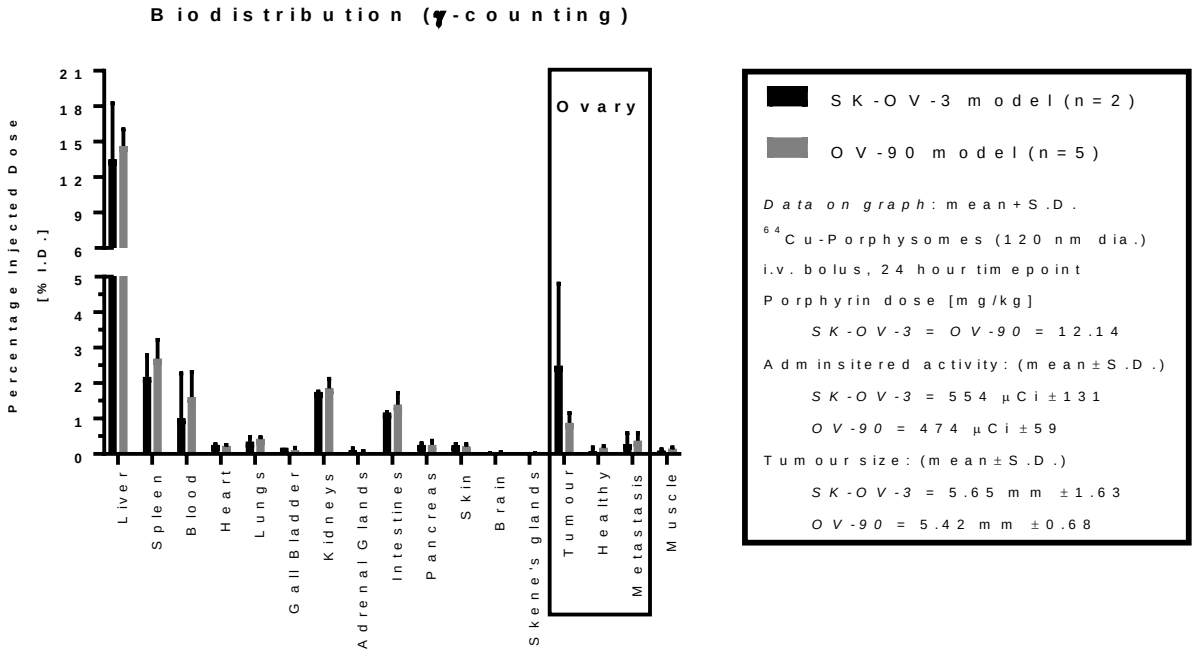

Figure 3: Biodistribution of ^{64}Cu-Porphysomes in the tissues of orthotopic xenograft models of human ovarian cancer. Each data point represents the mean + 1 standard deviation. ^{64}Cu activity was decay corrected to the time of injection and expressed as a percentage of the injected dose (%I.D.) normalized to tissue weight [g]. Difference in the %I.D. of the ovarian OV-90 tumour versus the contra-lateral healthy ovary was observed ($p = 0.0006$), but not for the ovarian SK-OV-3 tumour ($p = 0.2812$) owing to the small sample size ($n = 2$).

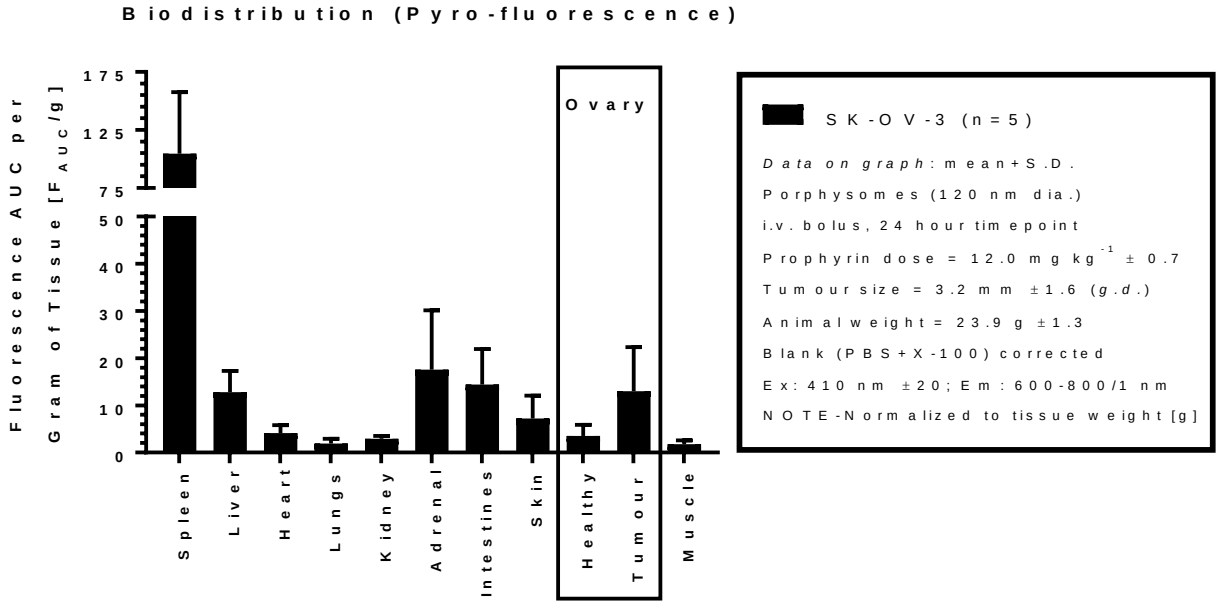

Figure 4: Biodistribution of Porphysomes in the tissues of orthotopic xenograft model of human ovarian cancer. Each data point represents the mean + 1 standard deviation. The area under the fluorescence spectrum curve (AUC) was integrated and blank corrected and normalized to tissue weight. No difference in the F_{AUC}/g of the ovarian SK-OV-3 tumour versus the contra-lateral healthy ovary was observed (p =0.05859).